Int. J. Electron. Commun. (AEÜ) 70 (2016) 1282–1287

Contents lists available at ScienceDirect

International Journal of Electronics and Communications (AEÜ)

journal homepage: www.elsevier.com/locate/aeue

Regular paper

Indefinite-permeability metamaterial lens with finite size for miniaturized wireless power transfer system

Yong Zhi Cheng [a,b,*], Ji Jin [a], Wen Long Li [b], Jun Feng Chen [c], Bin Wang [a], Rong Zhou Gong [b]

[a] Engineering Research Center for Metallurgical Automation and Detecting Technology Ministry of Education, Wuhan University of Science and Technology, Wuhan, Hubei 430081, China
[b] School of Optical and Electronic Information, Huazhong University of Science and Technology, Wuhan, Hubei 430074, China
[c] State Key Laboratory of Advanced Electromagnetic Engineering and Technology, Huazhong University of Science and Technology, Wuhan 430074, China

ARTICLE INFO

Article history:
Received 5 January 2016
Accepted 26 June 2016

Keywords:
Wireless power transfer
Indefinite-permeability
Metamaterial lens

ABSTRACT

A miniaturized wireless power transfer (WPT) system using indefinite-permeability metamaterial (IPMM) lens with finite size is proposed and investigated theoretically and experimentally. Theoretical simulations show that the IPMM lens outperforms isotropic negative metamaterial (NMM) lens in terms of coupling efficiency and lens size. A highly sub-wavelength IPMM operation at high frequency was designed, fabricated, and measured. The WPT experiments show that the efficiency can be enhanced significantly from 0.7% to 22.0% when the system is loaded with IPMM lens around 4 MHz. The further study shows that the IPMM lens can extend the operating distance of WPT by using an optimization approach.

1. Introduction

In recent years, wireless power transfer (WPT) has become more and more important due to its wide applications in consumer electronics, electrical vehicles and micro-implantable medical sensors. Many types of WPT have been proposed, such as electromagnetic (EM) induction [1], RF and microwave [2], and coupled electric fields [3]. Recently, the scheme based on near-field magnetic coupling has been designed [4]. Considering the balance of health, safety and efficiency, this scheme is one of the best solutions in a middle range distances. However, the current theory and experiment show that the energy transmission efficiency decreases sharply with the increasing of transmission distance [5]. This is because the relevant quasi-static field excited by source coil is evanescent and the near-field intensity decays exponentially away from the source. The rapidly reduced WPT efficiency is not qualified for practical devices. To overcome this problem, one approach is to increase mutual coupling strength of the source and receiver coils which can be achieved by the control of the near field distributions [6], especially, the field distribution can be modified by medium material lens.

Similar to the conventional high permeability magnetic materials that can guide magnetic flux and are used in transformers [7], left-handed materials (LHM) can be used as perfect lens by refocusing propagating waves and amplifying evanescent waves [8]. The LHM with both negative effective permittivity and permeability as a sub-class of metamaterials (MMs) have been investigated intensively due to their potential application [9–16]. Using negative-permeability MM lens to enhance the transmission efficiency in WPT has also proved to be an effective solution [17,18]. The initially proposed negative-permeability effective medium for WPT is three-dimensional (3D) MMs and realized by bulky volumetric structures. Further experimental studies show that the three principal values of the permeability tensor are unnecessary to be all negative for WPT [19–22]. By eliminating one (or two) negative component in the tensor, one (or two) resonant unit cell can be removed from each array element in the periodic artificial composite structure [23], which is usually named as indefinite-permeability MM (IPMM). The IPMM with the symmetric permeability tensors can be controlled to enhance evanescent waves with different wave numbers, which could be a desirable candidate for enhancing the WPT efficiency [24,25]. IPMM lens can reduce the fabrication complexity, the space between the magnetic resonators and the magnetic loss tangents, comparing with isotropic negative-permeability MM lens [25]. Previous researches have demonstrated that IPMM lens can be easily embedded into a WPT device and has better performance. The recent work of Huang et al. showed that the performance is closely related to the finite size of lens [6]. However, there is little literature about the studies on the finite size effects of IPMM lens and the realization of the high efficient WPTs embedded IPMM.

* Corresponding author at: Wuhan University of Science and Technology, No. 947#, Heping Road, Qingshan, Wuhan, Hubei 430081, China.
E-mail address: chengyz@wust.edu.cn (Y.Z. Cheng).

http://dx.doi.org/10.1016/j.aeue.2016.06.011
1434-8411/

In this work, we proposed an ultra-subwavelength IPMM for miniaturized WPTs at high frequency. The enhancement of mutual coupling between the two coils and the impact of the finite size of the IPMM lens were evaluated by theoretical simulation. Then we presented the design principles of the geometric structure and EM parameters that can achieve the best enhancement effect. Through this design, we can achieve the best enhancement effect for WPTs embedded IPMM. A highly sub-wavelength IPMM lens is proposed and realized on a thin slab using dual layer planar spiral resonators. The measured WPT efficiency is shown to be enhanced from 0.7% to 22.0% when the system is loaded with IPMM lens around 4 MHz. Furthermore, the proposed IPMM lens is demonstrated to extend transmission distance in coil axis directions and provide better transmission in a middle range distances.

2. Theoretical analyses and simulation

First of all, we theoretically studied the simple non-radiative WPT system that is made of two deeply sub-wavelength, high-Q coil resonators, such as spirals or solenoids. Here the source and receiver resonant coil is modeled by a finite size coil composed of a single turn of copper wire. A two-coil coupling system with MM lens is shown in Fig. 1(a). For the practical applications in the consumer electronics and wireless charging of implantable medical devices, the radius of source and receiver coils are selected as $r_1 = 4.5$ cm and $r_2 = 2$ cm, and the diameter of wire is 1 mm, respectively. Receiver coil is small enough to be used in most practical application such as cardiac pacemaker and cell phone charging. At the same time, we keep the transmitter coil bigger to get a further effective transmission distance. The mutual inductance M between the coils can be numerically analyzed by evaluating the magnetic flux in the receiver coil generated from the source coil. The M can be expressed as:

$$M = \frac{V_{\text{induced}}}{I_s} = \frac{-j\omega \int_{S_2} \vec{B}\vec{n}dA}{I_s} \tag{1}$$

where $\vec{B}$ is the magnetic flux density, $\vec{n}$ is the unit vector normal to the surface of S_2, and S_2 is the area encircled by the receiver coil. We can get the precise value of M in COMSOL Multiphysics based on the standard finite element method (FEM).

The use of a perfect lens which can capture the near-fields and refocus the flux at the receiver, thus enhancing the mutual coupling, is a fine approach for improving WPT efficiency. As shown in Fig. 1(a), a MM lens with finite diameter W and thickness L is placed in the middle of two coils. Since the dominant field components are magnetic and the WPT system operates in quasi-magneto static regime. It is expected that only the magnetic response of the slab will impact the near-field focusing, and thus only a magnetic component is assumed in this study. We consider the magnetic MM lens with diagonal material properties, where

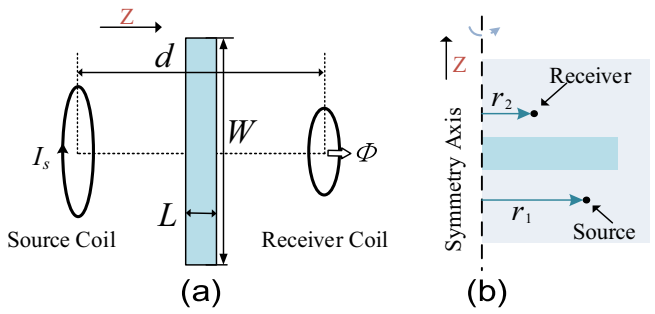

Fig. 1. (a) Two-coil coupling system with MM lens; (b) the equivalent axisymmetric 2D model.

the material properties can be represented as $\mu = [\mu_x, \mu_y, \mu_z]$, and ε is irrelevant and assumed as 1 for simplicity. The mutual inductance enhancement factor ρ defined in Ref. [6] can be used in our analysis to demonstrate how the mutual coupling of coils is affected by MM lens. The ρ is defined as the ratio between the mutual inductance enhanced with MM lens and the mutual inductance in vacuum, which can be written as:

$$\rho = \frac{M}{M_0} \tag{2}$$

where M_0 is the mutual inductance between the two resonant coils in free-space. The operation frequency is 4 MHz without otherwise specified; the transfer distance is $d = 10$ cm. Note the thickness of lens corresponds to the "perfect lens" condition, its thickness is $L = L_0 = d/2 = 5$ cm [8].

To demonstrate how the mutual coupling is affected by MM lens parameters of finite size, the enhancement factor ρ is analyzed with varying L and W. According to previous prediction [6], the enhancement factor ρ should produce periodic oscillation with increasing the value of W/L if we keep the permeability of MM as $\mu = [1, 1, -1 - 0.1j]$ and $\varepsilon = 1$.

According to the above theory analyses, we first investigate the effect of the varying diameter (W) when the thickness is kept as $L = d/2$. As shown in Fig. 2(a), there is a kind of similar damped oscillation and resonance peaks appear at $W = (n+1)d/2$, where n is a natural numbers. It can be observed that the first resonance peaks will appear, in this case, when $n = 1$, $W = d$. It also can be observed that the second resonance peaks will appear, in this case, when $n = 5$, $W = d$. The enhancement factor achieve the maximum when $W = d$. In another condition, if we keep lens diameter $W = d$ and change the value of lens thickness L, the enhancement factor achieve the maximum when $L = d/2$. The oscillations in the numerical result are due to the Fabry–Perot resonances (FPR), which result from the finite size of the IPMM lens and are enabled by the hyperbolic dispersion property of the indefinite medium [6]. In order to achieve the best reinforcing effect, we must ensure that $W = d$, $L = d/2$. Obviously, it is a frustrating result that the slab still occupies half of the space between the source and receiver.

A means of reducing the thickness profile of anisotropic negative permeability lens without changing the field mode in any manner has been proposed by applying techniques from transformation optics [6]. A spatial compression factor a is also introduced here to reduce the thickness of the IPMM lens. Based on previous study, in order to reduce the lens thickness, the permeability tensor is required to implement a reduction with $\mu_z = 1/a$ when the lens thickness is changed from L to L/a. We performed a parametric study, where the thickness of lens L ranges from 1 mm to 90 mm and the factor a varies from 50 to 0.5. In order to maintain the same performance as $L = L_0$, the loss must be scaled appropriately. Here, we scale the loss tangent of the IPMM lens in two different ways: $\sigma = 0.1/a$, $0.1/a^2$. The parametric study results for different scaling are shown in Fig. 3. As a contrast, the NMM lens with $\mu = -1 - 0.1j$ and $W = 0.2$ m was introduced in this parametric study. The results show that the intensity of mutual inductance increases exponentially when the thickness of the NMM slab increases with the overall distance between the source and receiver coils fixed at $d = 0.1$ m. The reason is that the closer the coils are placed to the NMM lens, the greater their coupling will be, where the local magnetic fields are very large. This means that forming an aplanatic point for perfect imaging is not necessarily required for WPT enhanced with NMM slab. For normal IPMM lens with $\mu = [1, 1, -1 - 0.1j]$ and $W = 0.1$ m, the field intensity in the receiver coil decreases exponentially as the thickness L decreases when $L \leqslant L_0$. While for the IPMM lens with $\sigma = 0.1/a^2$, the enhancement factor ρ approximately remains constant by using a method

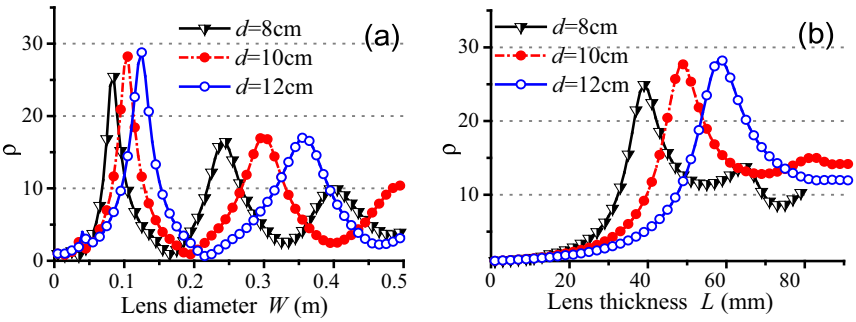

Fig. 2. The enhancement factor ρ obtained with MM lens as a function of (a) lens diameter W and (b) lens thickness L, when d = 8 cm,10 cm,12 cm.

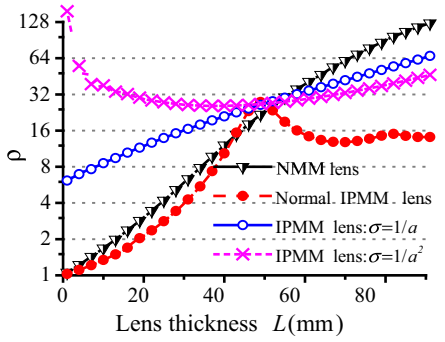

Fig. 3. The summary of enhancement ratio obtained with NMM lens and IPMM lens when the lens thickness changes. NMM lens has $\mu = -1 - 0.1j$ and W = 0.2 m; Normal IPMM lens has $\mu = [1, 1, -1 - 0.1j]$; IPMM lens with $\sigma = 1/a$ has $\mu = [1, 1, -1/a - 0.1/aj]$; IPMM lens with $\sigma = 1/a^2$ has $\mu = [1, 1, -1/a - 0.1/a^2J]$. The factor a is defined as L_0/L, where $L_0 = d/2$ = 5 cm. All IPMM lens has W = 0.1 m.

from transformation optics. In other words, we can achieve the same magnitude of coupling with a thinner IPMM lens without the necessary to ensure that the thickness of IPMM lens satisfy the "perfect lens" conditions. It is noteworthy that material loss needs to be well controlled.

From above theoretical results, the same order of magnitude enhancement of WPT efficiency can be expected for a WPT system equipped with an IPMM slab. Since the coils are inductive, parallel capacitors C_s = 6.08 nF and C_r = 16.09 nF were used to make source and receiver coils resonator at 4 MHz separately. Source coil was connected to an external voltage source with internal resistance R_s = 50 Ω. Correspondingly, receiver coil is also connected to a load resistance R_L = 50 Ω. The transmission efficiency η is defined as the ratio between the power delivered to the WPT system and the power delivered to the load resistance, which is given as:

$$\eta = \frac{P_{R_L}}{P_{\text{Source}} - P_{\text{Rs}}} \tag{3}$$

where the P_{Source} is the power of voltage source, P_{Rs} is the resistance loss of source and P_{R_L} is the power delivered to the load R_L. The relevant circuit parameters can be calculated directly in COMSOL Multiphysics.

The comparison of WPT efficiency for the conventional WPT system and the MM enhanced WPT systems when d = 0.1 m is shown in Fig. 4(a). At resonant frequency, the WPT efficiency is about 3.8% in free-space, 14.3% for NMM lens with $\mu = -1$–$0.1j$, W = 0.2 m, L = 5 cm and 29.8% for IPMM lens with μ = [1,1,–0.02–0.001j], W = 0.1 m, L = 1 mm. It is concluded that the higher enhancement of WPT efficiency can be achieved by using an IPMM slab, which should be designed carefully in the geometric dimensions and EM parameters. Because of different scale of loss, perhaps there are still some doubts about the excellent performance of IPMM lens discussed above. The same constant imaginary part 0.001j has been added to the permeability of both NMM lens and IPMM lens in next research. To examine the useful operation range of the WPT system, we simulate the transmission efficiency when d ranging from 4 to 16 cm as shown in Fig. 4(b). The WPT efficiency declines exponentially with the increase of transmission distance in free-space without any MM lens. Since we are not interested in creating a perfect image, the strict limit on the thickness of NMM slab determined by the "perfect lens" condition is unnecessary for the WPT application. In order to prevent the lens size too large, we chose d/4 as the thickness of NMM slab when distance increased. While the transmission efficiency in a wide distance range can be improved by using a NMM slab with varying thickness, it is unrealistic in actual applications. The performance improvement of using a NMM lens with $\mu = -1 - 0.001j$ and W = 0.2 m will become limited when the thickness L is fixed at 2 mm. Even if the thickness L of IPMM lens remains as thin as

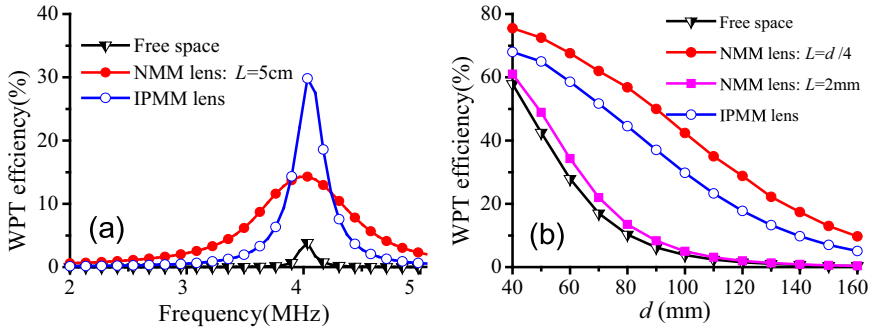

Fig. 4. Comparison of WPT efficiency for the conventional WPT system (free-space) and the metamaterial enhanced WPT systems: (a) WPT efficiency η vs frequency when d = 0.1 m and NMM lens has $\mu = -1 - 0.1j$, W = 0.2 m, and L = 5 cm; (b) WPT efficiency η vs distance and NMM lens has $\mu = -1 - 0.001j$, W = 0.2 m. In all cases, the IPMM lens has $\mu = [1, 1, -0.02 - 0.001j]$, W = 0.1 m, and L = 1 mm.

1 mm, the efficiency of transmission improved is still outstanding. The decline rate of the efficiency is also reduced compared with in free space, which means that the IPMM lens is also useful to extend the operating range of the WPT. Considering the size of lens and complexity of manufacture, IPMM lens is more appropriate in WPT applications.

The comparison of the H-field magnitude distributions with and without the presence of the IPMM slab is shown in Fig. 5. Due to symmetry, only half of the structure is demonstrated for the two cases. According to the previous study, there should exist some additional reflecting planes or standing waves on the slab surface, resulting from the effects related to the finite slab size [6]. As shown in Fig. 5, we indeed observed strong surface waves existing on both sides of the IPMM slab, which is responsible for the increased magnetic coupling [21]. From the magnetic field distributions, it is obvious that with the use of IPMM slab, much higher electrical energy can be coupled to the receiver coil.

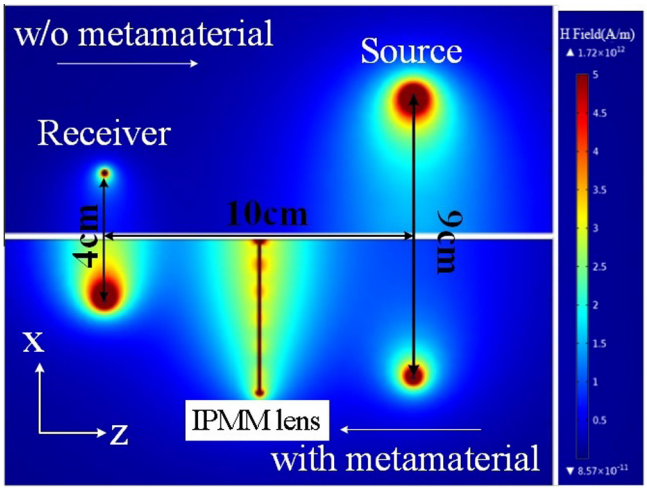

Fig. 5. Amplitude of the magnetic field distributions for a conventional WPT system (top) and an IPMM-enhanced WPT system with $\mu = [1, 1, 0.02 - 0.001j]$, $W = 0.1$ m, $L = 1$ mm (bottom) at 4 MHz when $d = 0.1$ m.

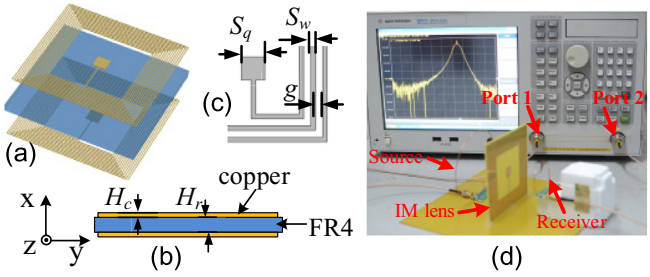

Fig. 6. (a) Schematic (exploded view) of the dual-layer square spiral metamaterial, (b) side view, (c) detailed view and its geometry parameters, (d) photograph of the WPT measured system.

3. IPMM for miniaturized WPT design and experiment

In order to further verify the above theory and simulation, one highly sub-wavelength IPMM was designed. As shown in Fig. 6(a), we choose a double-side square spiral linked with a square patch as the unit cell for IPMM. The outstanding characteristic of this structure has been proved by many previous researches [20,24–30]. In our design, each spiral on the substrate has 13 turns with strip width S_w of 1 mm and strip gap g of 0.6 mm, etched within an ultra-subwavelength dimension of 100 mm × 100 mm. The side length of the outer square is 98 mm, while that of the central capacitive pad S_q is 5 mm. All these copper structures are patterned on a substrate (FR4) with a relative permittivity of 4.5, a loss tangent of 0.02 and a thickness of $H_r = 1$ mm. All metallic components are modeled as copper with a conductivity of $\sigma = 5.8 \times 10^7$ S/m and a thickness of $H_c = 0.035$ mm.

It is convenient to simulate the unit cell of this kind of MM by using TEM waveguide method. A full wave frequency domain solver was performed for the next simulation. In our simulation, we force the plane wave to propagate in the z-direction with the H-field polarized along the x-direction and the E-field along the y-direction. Thus, we can figure out the complex scattering parameters S_{11} and S_{21}. Using a parameter retrieval procedure [31,32], the effective permeability of IPMM can be obtained from the reflection coefficient and the transmission coefficient. In this case, the simulated complex permeability is shown as red dashed lines in Fig. 7 (a) and (b). Next, we carried out the experiment by using an Agilent E5071C Vector Network Analyzer to determine the effective permeability of IPMM and WPT efficiency. With a method proposed in Ref. [30], the effective permeability can be obtained and is shown as black solid lines in Fig. 7(a) and (b). From the Fig. 7, we can see the measured and simulated permeability values are $\mu = -1.6 - 0.37j$ and $\mu = -0.9 + 0.26j$ at 4 MHz. It is clear that the results obtained from measurement agree well with simulation. Obviously, the values of the relative permeability nearly satisfy the requirement of the IPMM condition that enhance the WPTs efficiency.

A photograph of the measured system is shown in Fig. 6(d). The source and receiver coils with capacitance compensation were connected to port 1 and port 2 of the network analyzer. The received electric field component E_z at the location of port 2 is converted to voltage for the calculation of the scattering parameters S_{11} and S_{21}. Then the efficiency of the WPT system is calculated as $|S_{21}|^2/(1 - |S_{11}|^2)$ [25]. The comparison of simulated and measured

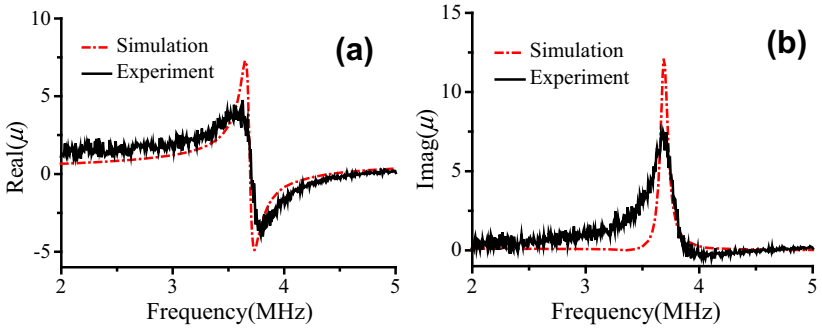

Fig. 7. The effective complex permeability: (a) the real part and (b) imaginary part.

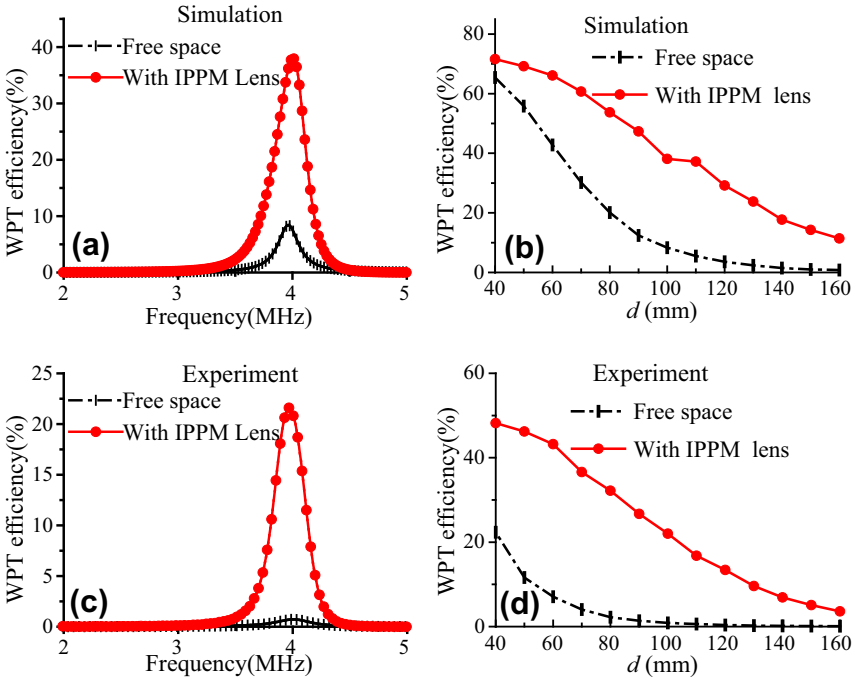

Fig. 8. Comparison of WPT efficiency with loading and unloading designed IPMM lens by simulation and experiment: (a, c) WPT efficiency η vs frequency of when d = 0.1 m; (b, d) WPT efficiency η vs distance.

efficiency of the WPT system with and without IPMM slab is given in Fig. 8(a, c) where d = 10 cm. The experimental results are in reasonable agreement with the simulations. However, the values of the WPT efficiency of measurements are somewhat discrepancy with the simulations, which maybe caused by fabrication tolerances and the imperfection in measurements. Due to the mutual inductance introduced by the IPMM slab, the simulated maximum efficiency could rise from 8% to 38%, while the measured one rise from 0.7% to 22%. Because the Q-factor of the actual coils is smaller than the theoretical value, the values of efficiency measured in free-space are lower than those of simulation. Fig. 8(b, d) shows the comparison of simulated and measured WPT efficiency with and without the presence of the IPMM slab at the frequency of 4 MHz versus varies distance. With the increasing of the transmission distance, both simulation and experiment results exhibit that the decrease rate of the efficiency with IPMM lens is lower than that without IPMM lens.

4. Conclusion

In summary, we present the numerical and experimental study of a miniaturized WPT system based on IPMM lens with finite size. We analyzed the enhancement mechanism of IPMM lens compared with the NMM lens in numerical simulation by evaluating of the enhancement factor ρ of mutual coupling. The results show that the IPMM lens can outperform NMM lens if we make use of Fabry–Perot resonances resulted from finite size of IPMM lens and techniques from transformation optics. Then, an IPMM lens with finite size working at 4 MHz was designed, fabricated, and measured to verify the previous prediction. With the proposed IPMM lens, the WPT efficiency can be effectively enhanced from 0.7% to 22% when d = 10 cm. With the increasing the distance of coils, the decline rate of the efficiency is also reduced compared to that without indefinite MM lens. The experimental result agrees well with the simulation. This miniaturization WPT system with IPMM lens should have potential applications in the consumer electronics and wireless charging of implantable medical device.

Acknowledgments

This work is supported by the Joint Funds of the National Natural Science Foundation of China (Grant No. U1435209) and the Youth science and technology backbone cultivation plan project of the Wuhan University of Science and Technology (Grant No. 2016xz010).

References

[1] Brown WC. The history of power transmission by radio waves. IEEE Trans Microw Theory Tech 1984;32:1230–42.
[2] Boys J, Covic G, Green AW. Stability and control of inductively coupled power transfer systems. IEE P-Electr Power Appl 2000;147:37–43.
[3] Leyh G, Kennan M. Power symposium, NAPS '08. 40th North American. p. 1.
[4] Kurs A, Karalis A, Moffatt R, Joannopoulos JD, Fisher P, Soljačić M. Wireless power transfer via strongly coupled magnetic resonances. Science 2007;317:83–6.
[5] Ahn D, Hong S. A study on magnetic field repeater in wireless power transfer IEEE Trans. Ind Electron 2013;60:360–71.
[6] Huang D, Urzhumov Y, Smith DR, Teo KH, Zhang J. Magnetic superlens enhanced inductive coupling for wireless power transfer. J Appl Phys 2012;111:064902.
[7] Mater Hasegawa R. Applications of amorphous magnetic alloys. Sci Eng A 2004;375–377:90–7.
[8] Pendry JB. Negative refraction makes a perfect lens. Phys Rev Lett 2000;85:3966.
[9] Smith DR, Padilla WJ, Vier D, Nemat-Nasser SC, Schultz S. Composite medium with simultaneously negative permeability and permittivity. Phys Rev Lett 2000;84:4184.
[10] Cheng YZ, Yang HL, Nie Y, Gong RZ, Cheng ZZ. Investigation of negative index properties of planar metamaterials based on split-ring pairs. Appl Phys A 2011;103:989–94.
[11] Fang N, Lee H, Sun C, Zhang X. Sub–diffraction-limited optical imaging with a silver superlens. Science 2005;308:534.
[12] Schurig D, Mock JJ, Justice BJ, Cummer SA, Pendry JB, Starr AF, Smith DR. Metamaterial electromagnetic cloak at microwave frequencies. Science 2006;314:977.
[13] Cheng YZ, Gong RZ, Cheng ZZ. A photoexcited broadband switchable metamaterial absorber with polarization-insensitive and wide-angle absorption for terahertz waves. Opt Commun 2016;361:41–6.
[14] Cheng YZ, Wu CJ, Cheng ZZ, Gong RZ. Ultra-compact multi-band chiral metamaterial circular polarizer based on triple twisted split-ring resonator. Prog Electromagn Res 2016;115:105–13.

[15] Liu JP, Cheng YZ, Nie Y, Gong RZ. Metamaterial extends microstrip antenna. Microwave RF 2013;52(12):69–73.
[16] Fan Y, Cheng YZ, Nie Y, Wang X, Gong RZ. An ultrathin wide-band planar metamaterial absorber based on fractal frequency selective surface and resistive film. Chin Phys B 2013;22(6):67801.
[17] Choi J, Seo C. High-efficiency wireless energy transmission using magnetic resonance based on negative refractive index metamaterial. Prog Electromagn Res 2010;106:33–47.
[18] Wang B, Teo KH, Nishino T, Yerazunis W, Barnwell J, Zhang J. Experiments on wireless power transfer with metamaterials. Appl Phys Lett 2011;98:254101.
[19] Fan Y, Li L, Yu S, Zhu C, Liang C-H. Experimental study of efficient wireless power transfer system integrating with highly subwavelength metamaterials. Prog Electromagn Res 2013;141:769–84.
[20] Wang B, Yerazunis W, Teo KH. Wireless power transfer: metamaterials and array of coupled resonators. Proc IEEE 2013;101:1359–68.
[21] Ranaweera A, Duong TP, Lee JW. Experimental investigation of compact metamaterial for high efficiency mid-range wireless power transfer applications. J Appl Phys 2014;116:043914.
[22] Rajagopalan A, RamRakhyani AK, Schurig D, Lazzi G. Improving power transfer efficiency of a short-range telemetry system using compact metamaterials. IEEE Trans Microwave Theory Tech 2014;62:947–55.
[23] Chen WC, Bingham CM, Mak KM, Caira NW, Padilla WJ. Extremely subwavelength planar magnetic metamaterials. Phys Rev B 2012;85:201104.
[24] Smith DR, Schurig D. Electromagnetic wave propagation in media with indefinite permittivity and permeability tensors. Phys Rev Lett 2003;90 (7):077405.
[25] Zhao Y, Leelarasmee E. Controlling the resonances of indefinite materials for maximizing efficiency in wireless power transfer. Microwave Opt Technol Lett 2014;56:867.
[26] Urzhumov Y, Chen W, Bingham C, Padilla W, Smith DR. Magnetic levitation of metamaterial bodies enhanced with magnetostatic surface resonances. Phys Rev B 2012;85:054430.
[27] Roberts D, Kundtz N, Smith D. Optical lens compression via transformation optics. Opt Express 2009;17(9):16535–42.
[28] Li L, Fan Y, Yu S, Zhu C, Liang C. Design, fabrication, and measurement of highly sub-wavelength double negative metamaterials at high frequencies. J Appl Phys 2013;113:213712.
[29] Wu Q, Li Y, Gao N, Yang F, Chen Y, Fang K, Zhang Y, Chen H. Wireless power transfer based on magnetic metamaterials consisting of assembled ultra-subwavelength meta-atoms. Euro Phys Lett 2015;109:68005.
[30] Lipworth G, Ensworth J, Seetharam K, Huang D, Lee JS, Schmalenberg P, Nomura T, Reynolds MS, Smith DR, Urzhumov Y. Magnetic metamaterial superlens for increased range wireless power transfer. Sci Rep 2014;4:3642.
[31] Smith D, Vier D, Koschny T, Soukoulis C. Electromagnetic parameter retrieval from inhomogeneous metamaterials. Phys Rev E 2005;71:036617.
[32] Chen WC, Bingham CM, Mak KM, Caira NW, Padilla WJ. Extremely subwavelength planar magnetic metamaterials. Phys Rev B 2012;85 (20):201104.